CONFIDENTIAL EXTENDED ABSTRACT.
DO NOT DISTRIBUTE ANYWHERE.

The 20th Meeting on Image Recognition and Understanding

Non-rigid registration of serial section images by blending 2D rigid transformations

Takehiro Kajihara[1,a)] Takuya Funatomi[1] Haruyuki Makishima[2] Takahito Aoto[1]
Hiroyuki Kubo[1] Shigehito Yamada[2] Yasuhiro Mukaigawa[1]

1. Introduction

The 3D structure of biological tissue is crucial to gain structural insights for physiology and pathology. Histological section images have higher resolution compared to MR and CT image. Therefore, a 3D model reconstructed from histological section images gives us more detailed structural information. However, histological section images have non-rigid deformation (e.g. tissue stretching, tearing) caused by the sectioning process of the tissue. This deformation causes a gap between neighbor images. Therefore, image registration is required to reduce the gap for reconstructing 3D model from histological sections.

In the registration process, we obtain appropriate transformation that maps the source image onto the target one. Several popular methods in registration for histological images [1], [2] are based on the Free-form deformations (FFD) with B-spline interpolation. FFD estimates displacement at control points and calculates the displacement at every point using interpolation. However, the descriptive power of the deformation highly depends on the resolution of the grid of the control points [3].

In this paper, we propose a novel non-rigid registration method that extends FFD. The proposed method has three improvements on the displacement field. First, each control point has a rigid transformation (translation and rotation) where a control point of FFD has a displacement (translation). Second, the interpolation method is also modified as a weighted blending of rigid transformations rather than taking a weighted sum of translational vectors. Third, the control points are defined not on a grid, but on several local regions according to the pattern

1 Graduate School of Information Science, Nara Institute of Science and Technology
2 Graduate School of Medicine, Kyoto University
a) kajihara.takehiro.kj7@is.naist.jp

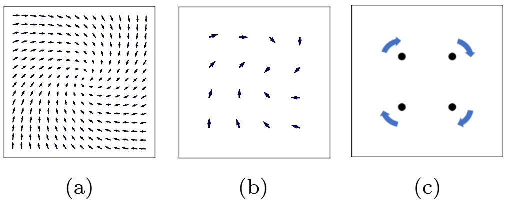

Fig. 1: Representation of deformation: (a) Displacement in each pixels, (b) Displacement field of FFD. Arrow: displacement, (c) Transformation field of the proposed method. Dot: control point, Arrow: rigid transformation.

on the image. The proposed method calculates transformation field that defines a rigid transformation at every point by blending the rigid transformations at the control points. Since every point may have an individual rigid transformation, the transformation field can describe non-rigid deformation on the whole image.

For example, if an image has rotational transform as shown in Fig. 1–a, it forms complex displacement field. FFD represents the deformation by using control points defined on a grid as shown in Fig. 1–b. The estimated transformation becomes coarse from a low-resolution grid of the control points. Thus, dense control points are required to represent the rotation more accurately. However, it is not stable to correctly estimate the translations on a fine grid due to such staining variation, thus it would lead registration faults. Meanwhile, the proposed method can describe complex non-rigid deformation from a smaller number of control points than FFD, thus it is more robust.

2. Proposed Method

The proposed method consists of five steps as shown in Fig. 2. First, we extract feature points for the images to be processed and calculates matching of them. Next, we define local regions each of which has small non-rigid

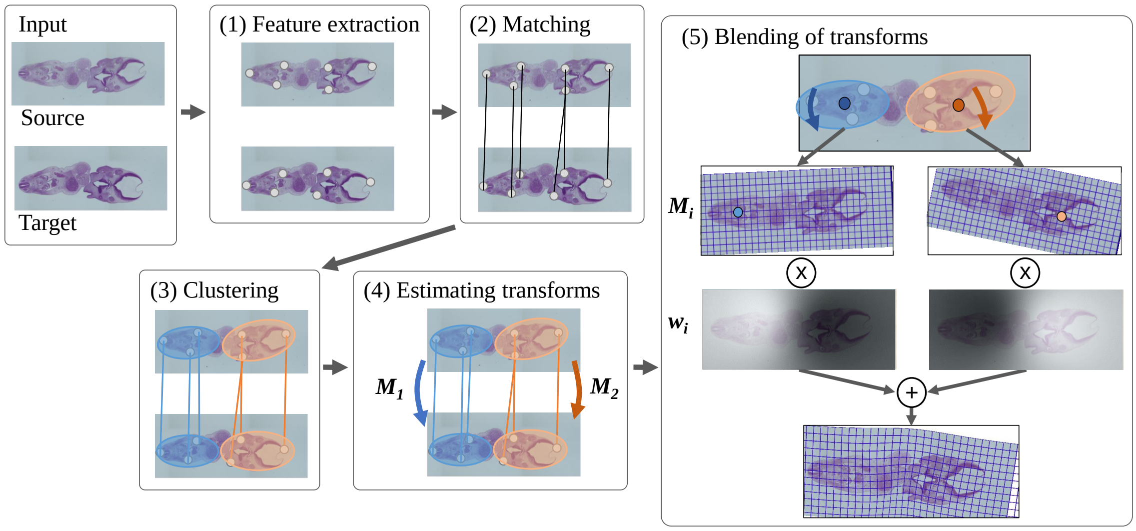

Fig. 2: Overview of non-rigid registration of the proposed method: Using source and target images as input, the method (1) extracts feature keypoint, (2) matches them, (3) conducts clustering of the matching (the case for $k = 2$ is shown), and (4) estimates rigid transformation $\boldsymbol{M_i}$ in each cluster. The transformation field is computed by (5) blending the transformations $\boldsymbol{M_i}$ with the weight w_i to represent a non-rigid deformation.

deformation, then estimate a rigid transformation in each cluster. Finally, we compute a transformation field. The following sections explain these steps in details.

2.1 Preprocessing

The proposed method estimates rigid transformations based on keypoint detection and feature matching as the previous methods of rigid registration do. Though any method can be used for keypoint detection and feature description, we adopt AKAZE (Accelerated-KAZE) [4]. By applying the method for the source and target images, two sets of keypoints are acquired (Fig.2 (1)). Between them, feature matching is performed by using Hamming distance and brute-force matching (Fig.2 (2)).

As a preprocessing of the keypoint detection, histogram equalization is performed to compensate the staining variations. The method also extracts the tissue region to reduce meaningless keypoints due to the noises in the background. It also removes obviously incorrect matches of which the positions in the source and target images are too far by assuming that the non-rigid deformation is not so large. Indeed, even if there is no deformation, the images are also affected by rotation and translation, which are referred as rigid transformation, as occurred in the capturing process. The differences due to the rigid transformation need to be preliminary eliminated, so the algorithm first estimates the rigid transformation between the source and target images using the whole set of the matched feature points. The rigid transformation matrix $\boldsymbol{R}$ is estimated using RANSAC (Random Sample Consensus) algorithm [5] as the existing methods do. The position $\boldsymbol{p}^s$ of a pixel on the source image is transformed onto $\boldsymbol{p}^{s'}$ by

$$\boldsymbol{p}^{s'} = \boldsymbol{R}\boldsymbol{p}^s. \tag{1}$$

Here, $\boldsymbol{p}^s$ and $\boldsymbol{p}^{s'}$ are homogeneous coordinate.

2.2 Estimating local transformations

We assume that each non-rigid deformation occurred in each local region which is in a neighborhood and has similar RGB value. According to the assumption, we perform k-means clustering of the keypoints (Fig.2 (3)). For the feature space of the k-means, we use normalized coordinates and RGB value of the keypoint. Then, we define a control point $\boldsymbol{v_i}$ as the center of the i-th cluster of the source image. Using the keypoints in each cluster, a rigid transformation $\boldsymbol{M_i}$ is also estimated using RANSAC as well as the above (Fig.2 (4)).

2.3 Calculating transformation field by blending local rigid transformations

The proposed method estimates a transformation field that has a rigid transformation at each pixel by blending the rigid transformations $\{\boldsymbol{M_i}\}$ (Fig.2 (5)). Blending rigid transformations is studied in computer graphics field. One of the simplest methods represents rigid transformation $\boldsymbol{M_i}$ in matrix form, takes weighted sum for each element, and normalizes the resultant matrix to be a rigid transformation. However, it is well known that some artifacts would occur such as candy wrapper effect.

As for blending 3D transformations, DLB (Dual quaternion Linear Blending) and DIB (Dual quaternion Iterative Blending) are proposed to overcome the artifact [6]. For 2D, anti-commutative dual complex and its application to DLB have been proposed [7]. Here, we extend DIB to a 2D case as DCIB (Dual Complex Iterative Blending). The proposed method transforms a pixel $\boldsymbol{p}^{s'}$ in the transformed source image onto $\boldsymbol{p}^{s''}$ by the following equation.

$$\boldsymbol{p}^{s''} = \mathbf{F}(\mathbf{w}(\mathbf{p}^{\mathbf{s}'}), \mathbf{M})\mathbf{p}^{\mathbf{s}'}, \tag{2}$$

$$\boldsymbol{w}(\boldsymbol{p}^{\boldsymbol{s}'}) = [w_1(\boldsymbol{p}^{s'}), ..., w_k(\boldsymbol{p}^{s'})]^\top, \tag{3}$$

$$\boldsymbol{M} = [\boldsymbol{M_1}, ..., \boldsymbol{M_k}]^\top, \tag{4}$$

where $w_{i\in[1,k]}$ are the blending weights, $\boldsymbol{M_{i\in[1,k]}}$ are the rigid transformations, k is the number of clusters, and $\mathbf{F}$ is a blending of transformations by DCIB.

We empirically set the weight w_i at a pixel $\boldsymbol{p}$ according to Euclid distance from $\boldsymbol{p}$ to a control point $\boldsymbol{v}_i$ as follows.

$$t_i(\boldsymbol{p}) = \frac{1}{\|\boldsymbol{p} - \boldsymbol{v}_i\|_2^2}, \tag{5}$$

$$w_i(\boldsymbol{p}) = \frac{t_i(\boldsymbol{p})}{\sum_i t_i(\boldsymbol{p})}, \tag{6}$$

Since the weights need to be convex ($w_i \geq 0, \sum_i w_i = 1$) we normalize the weights to meet the conditions, to guarantee the convergence of DIB. Each pixel has the different rigid transformation because each pixel has individual weights. Thus, transformation field represents non-rigid deformation in the whole image.

3. Experiment

We experimentally present that the proposed method is applicable to non-rigid registration. For this purpose, we use images of a histological section. The samples used in this experiment are a part of the Kyoto Collection of Human Embryos maintained in the Congenital Anomaly Research Center, Kyoto University [8]. This study was approved by the Ethics Committee of the Graduate School of Medicine and Faculty of Medicine, Kyoto University (approval nos. R0316 and R0347). The serial sections have about 10 micrometers of thickness, and a microscopy is used to capture the images with about 5 micrometers of resolution. For the evaluation, we select four specimens from the collection and randomly select twenty pairs of two neighboring images from each specimen.

We compare our method with one of the existing non-rigid registration methods, bUnwarpJ (elastic registration using B-spline) [1]. Figure 3 presents the target image (a), the source image (b), and results of registration (c)–(e). We show the results of samples with low (the first row) and high (the third row) variations of staining. The second and fourth rows present the overlay of the registration result and the target image.

Even though the number of the control points used in our method is much fewer than in bUnwarpJ, the proposed method achieved better performance for samples with high staining variation where bUnwarpJ has large deformation error as shown in the bottom row of Fig. 3. This result indicates the robustness of our methods.

Next, we compared the registration methods in various settings to investigate the effect of a number of control points. We evaluate registration accuracy by Jaccard Index (JI) [9], which represents the overlap ratio of extracted tissue regions in two corresponding images. The accuracy with various settings is presented in Fig 4. bUnwarpJ required a lot of control points (8×8) for better accuracy, while the proposed method only required 4 clusters to achieve almost the same accuracy.

Figure 5 shows the direct comparison of the accuracy of bUnwarpJ and the one of our method using the same number of control points. One can see that our method achieved similar or much better accuracy than bUnwarpJ in most samples as the most plot points are higher than the diagonal line.

4. Conclusion

This paper proposed a novel non-rigid registration method that establishes transformation field. The proposed method estimates rigid transformation in local regions and blending them to interpolate the transformations at every pixel. Comparing to the distance field, our transformation field can describe much complex deformation with a smaller number of control points. The experiments show that the proposed method represents non-rigid deformation by using a small number of control points and is more robust compared to a popular existing method. As future work, it is required to decide the number of local regions and blending weights automatically.

References

[1] I. Arganda-Carreras, C.O.S. Sorzano, R. Marabini, J.M. Carazo, C. Ortiz-deSolorzano, and J. Kybic, “Consistent and elastic registration of histological sections using vector-spline regularization,” CVAMIA: Computer Vision Approaches to Medical Image Analysis, pp.85–95, 2006.

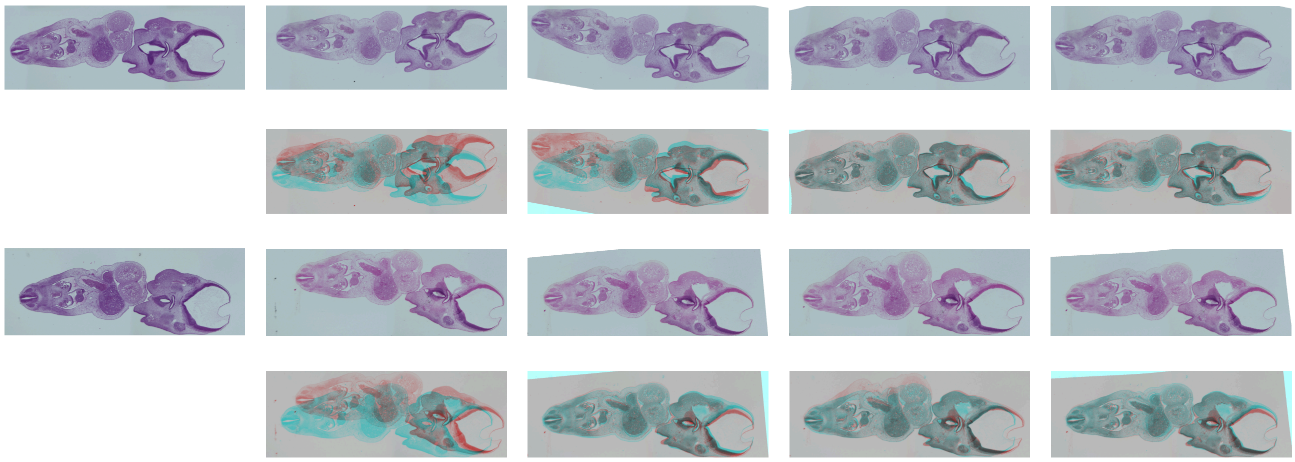

(a) Target (b) Source (c) Rigid (d) bUnwarpJ (e) Ours

Fig. 3: Registration of histological section images: (a) Target image, (b) Source image, (c) Results of rigid registration, (d) Non-rigid Registration by bUnwarpJ (deformation grid $= 8 \times 8$), (e) Proposed non-rigid registration (cluster number $k = 8$). The first and third rows show registration images. The second and fourth rows show the target image (a) in blue and each (a–e) in red.

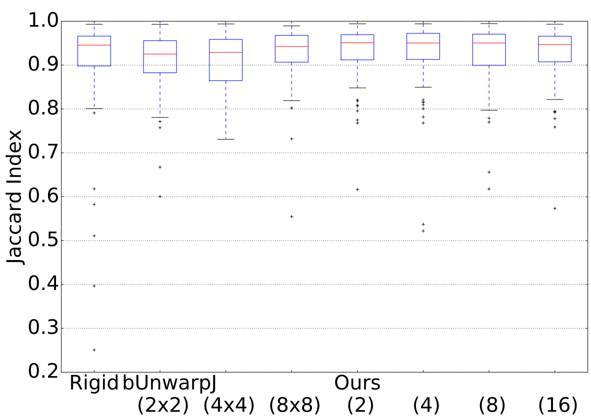

Fig. 4: Accuracy of registration by JI: JI of registration images in each methods, rigid registration (Rigid), bUnwarpJ (bUn) and our method (Ours) in various settings. In bUnwarpJ, $(n \times n)$ represents deformation grid of $n \times n$ intervals. In our method, (n) represents the number of control points n.

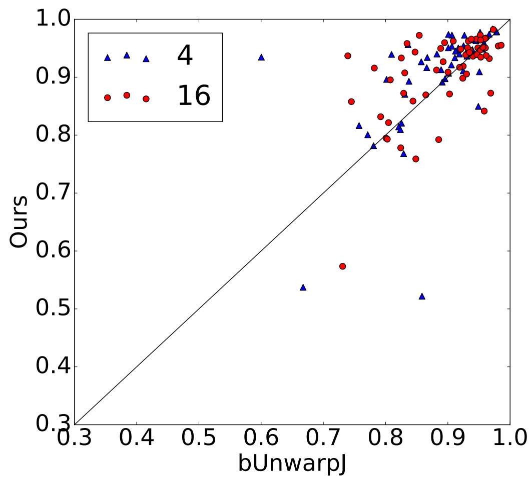

Fig. 5: Accuracy comparison of bUnwarpJ and our method with the same number of control points for the same image pair. x-axis shows JI of bUnwarpJ with deformation grid intervals is $2 \times 2 = 4$ or $4 \times 4 = 16$. y-axis shows JI of our method with control points is 4 or 16.

[2] C. Wang, E.B. Gosno, and Y. Li, "Fully automatic and robust 3D registration of serial-section microscopic images," Scientific Reports, pp.1–14, 2015.

[3] D. Rueckert, P. Aljabar, R.A. Heckemann, J.V. Hajnal, and A. Hammers, "Diffeomorphic registration using B-splines.," Medical image computing and computer-assisted intervention : MICCAI, International Conference on Medical Image Computing and Computer-Assisted Intervention, vol.9, no.Pt 2, pp.702–9, 2006.

[4] P. Alcantarilla, J. Nuevo, and A. Bartoli, "Fast Explicit Diffusion for Accelerated Features in Nonlinear Scale Spaces," Procedings of the British Machine Vision Conference, pp.13.1–13.11, 2013.

[5] M.A. Fischler and R.C. Bolles, "Paradigm for Model," Communications of the ACM, vol.24, no.6, pp.381–395, 1981.

[6] L. Kavan, S. Collins, J. Žára, and C. O'Sullivan, "Geometric skinning with approximate dual quaternion blending," ACM Transactions on Graphics, vol.27, pp.1–23, 2008.

[7] G. Matsuda, S. Kaji, and H. Ochiai, "Anti-commutative Dual Complex Numbers and 2D Rigid Transformation," Mathematical Progress in Expressive Image Synthesis I, pp.131–138, 2014.

[8] S. Yamada, C. Uwabe, S. Fujii, and K. Shiota, "Phenotypic variability in human embryonic holoprosencephaly in the kyoto collection," Birth Defects Research Part A: Clinical and Molecular Teratology, vol.70, no.8, pp.495–508, 2004.

[9] T. Rohlfing, "Image similarity and tissue overlaps as surrogates for image registration accuracy: Widely used but unreliable," IEEE Transactions on Medical Imaging, vol.31, no.2, pp.153–163, 2012.